**Revised manuscript**

# Thermochronology and the three-dimensional cooling pattern of a granitic pluton: An example from the Toki granite, Central Japan.

Takashi Yuguchi[1]*, Kenji Amano[2], Tadahiko Tsuruta[1,3], Tohru Danhara[4] and Tadao Nishiyama[3]

[1]Mizunami Underground Research Laboratory, Geological Isolation Research and Development Directorate, Japan Atomic Energy Agency, 1-64, Yamanouchi, Akeyo, Mizunami, Gifu, 509-6132, Japan.
[2]Horonobe Underground Research Center, Geological Isolation Research and Development Directorate, Japan Atomic Energy Agency, 1-8, Miyazono, Horonobe, Teshio, Hokkaido, 098-3207, Japan.
[3]Department of Earth and Environmental Sciences, School of Science, Graduate School of Science and Technology, Kumamoto University, 2-39-1, Kurokami, Kumamoto 860-8555, Japan.
[4]Kyoto Fission-Track Co., Ltd, 44-4, Minamitajiri, Omiya, Kita-ku, Kyoto, 603-8832, Japan.

* Corresponding author. Tel.: +81 572 66 2244 / Fax: +81 572 66 2245
*E-mail address*: yuguchi.takashi@jaea.go.jp (T. Yuguchi)

**Abstract**

The three dimensional spatial variations in the cooling pattern of the Toki granitic body, a zoned pluton in Central Japan, have been evaluated quantitatively by thermochronology using cooling age determination based on the different closure temperatures for target mineral species. The Toki granite has hornblende K-Ar ages of about 74.3±3.7 Ma (n = 2; closure temperature of 510±25 $^{o}$C), biotite K-Ar ages of 78.5±3.9 to 59.7±1.5 Ma (n = 33; 300±50 $^{o}$C), and zircon fission-track ages of 75.6 ±3.3 to 52.8±2.6 Ma (n = 44; 240±50 $^{o}$C). The spatial variation in the biotite K-Ar age is similar to that in the zircon fission-track age in samples collected from 11 boreholes and seven outcrop sites in the Toki granite, indicating that cooling was effectively from the roof and also from the northwest margin. This cooling pattern shows a strong correlation with the Alumina Saturation Index (ASI) distribution of the body. Larger ASI values correspond to earlier and more rapid cooling after emplacement and smaller value to slower cooling. Toki granite was effectively cooled from the peraluminous regions where assimilation of country sedimentary rock was most extensive.

KEYWORDS: Cooling process; Granitic pluton; Thermochronology; K-Ar dating; Fission-track dating; Toki granite

## Introduction

Thermochronology, which is based on plural dating methods utilizing different closure temperatures for target minerals, is a powerful tool for quantifying a cooling process of a granitic body. The cooling process such as direction of heat release and the cooling rate will give important information about the size and configuration of the pluton in the crust and also about the depth of the intrusion, some of which can be evaluated independently by geological and petrological methods. Knowledge of the cooling also has potential practical application in understanding the distribution of fractures (e.g. cooling joints) and the hydrothermal circulation in a pluton.

The application of thermochronometry to one particular sample (i.e. one particular position) inside the granite can clarify the "sub-solidus temperature-time path" that the plutonic rock has undergone. Additionally, the application of thermochronology to plural samples widely-collected from a granite, i.e. "multi-sampling thermochronology" can reveal the three-dimensional cooling pattern of a pluton through the spatiotemporal change of temperature inside the body. There has been a lot of discussion about cooling rate and uplift history of granitic bodies based on thermochronology (e.g. Dodson and McClelland 1985; Hurford 1986; Yuhara and Kagami 1995; Tsuchiya and Fujino 2000; Umeda et al. 2001; Zhao et al. 2004). However, there have been few attempts to clarify the three-dimensional cooling pattern of an individual pluton. Only a few studies based on "multi-sampling thermochronology" investigated vertical (e.g. Harayama 1992; Harayama 1994; Eby et al. 1995) or horizontal variations (e.g. Bando et al. 2003; Oikawa et al. 2006) of the cooling process. Harayama (1992 and 1994) described vertical variations in cooling rate of the Plio-Pleistocene Takidani Granodiorite, Central Japan. He showed that there was a difference in the cooling rate between higher and lower levels in the granodiorite based on biotite, K-feldspar and hornblende K-Ar dating and zircon fission-track dating for four samples collected from various levels. Oikawa et al. (2006) described the horizontal variations in the cooling pattern of the Miocene Ichifusa-yama Granodiorite, Kyushu, Japan. They suggested an unusual manner of cooling such that the rate of cooling from 300 $^{o}$C to 100 $^{o}$C in the central part of the body was about 100 $^{o}$C / m.y., i.e., faster than that in the periphery, based on biotite K-Ar, zircon fission-track and apatite fission-track dating for four samples. Oikawa et al. (2006) concluded that the influence of paleotopography resulted in the anomalous cooling pattern inside the body.

This study investigated the three-dimensional cooling pattern in a granitic body, the Toki granite, Central Japan (Fig. 1), by employing "multi-sampling thermochronology". The Toki granite is a good example for such a study because the petrography were already described by Yuguchi et al. (2010) and the rock mass is clarified to have solidified as a zoned pluton of the Late Cretaceous in age. Nineteen boreholes were drilled in the Toki granite (Fig. 2A) by Japan Atomic Energy Agency (JAEA), for the 'Regional Hydrological Study (Japan Nuclear Cycle Development Institute 2000)' and for the 'Mizunami Underground Research Laboratory Project (Japan Nuclear Cycle Development Institute 2002)'. The borehole lengths range from about 500 m to about 1300 m. Samples collected from 11 boreholes and seven outcrops in the Toki granite display spatial variations in mineral ages within the body in three dimensions (Fig. 2A), which can be related to difference in cooling rate of the magmatic body. Availability of these samples allows placing accurate constraints on the three-dimensional cooling process of the Toki granite using "multi-sampling thermochronology".

Good indicators of low-temperature closure thermochronometry in granite include biotite K-Ar dating and zircon fission-track dating. The data are mapped according to horizontal location and vertical elevation within the body. The cooling patterns of the Toki granite at the temperature of biotite K-Ar closure ($300 \pm 50$ $^{o}$C) and zircon fission-track closure ($240 \pm 50$ $^{o}$C) stages, respectively, are evaluated based on the spatial variations in the data.

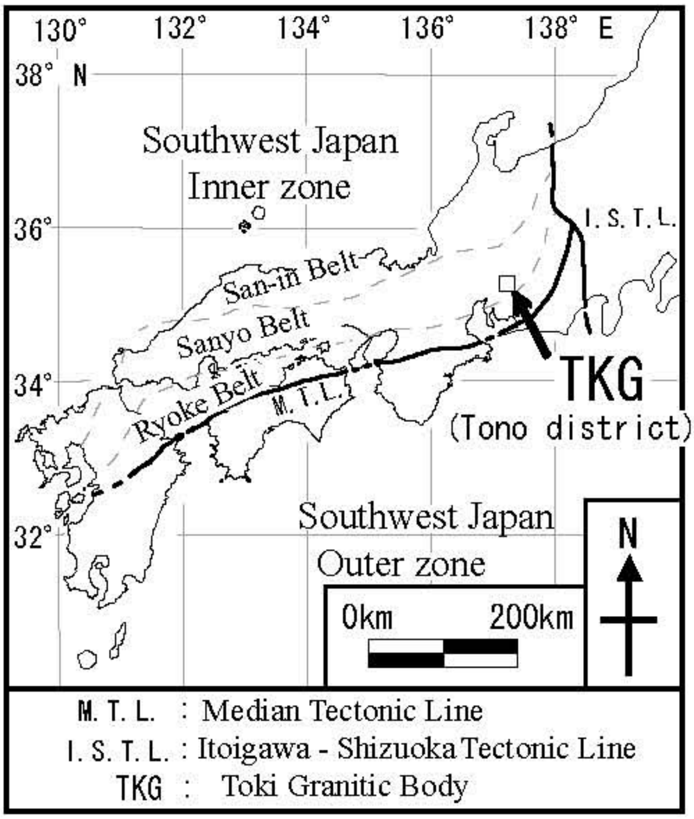


**Fig. 1** Location map showing the Toki granite (Tono district; square symbol) in Central Japan, together with the distribution of San-in, Sanyo and Ryoke Belts in the Inner Zone of Southwest Japan, after Ishihara and Chappell (2007).

**The Toki granite**

The Southwest Japan is divided by the Median Tectonic Line (M.T.L.) into Inner and Outer Zones (Fig. 1). Igneous rocks of Cretaceous to Palaeogene age in the Inner Zone of Southwest Japan occur in the parallel, northeast-southwest oriented Ryoke, Sanyo and San-in Belts (Ishihara 2003). The Toki granite in the Tono district, Gifu, Central Japan, is one of the Late Cretaceous plutonic bodies of the Sanyo Belt (Ishihara and Chappell 2007; Fig. 1), and has been dated at 68.3±1.8 Ma (monazite chemical Th-U-total Pb isochron method (CHIME) : Suzuki and Adachi 1998) and 72.3±3.9 Ma (whole-rock Rb-Sr: Shibata and Ishihara 1979).

The Toki granite is a nearly circular stock, with 14×12 $km^2$ in areal extent (Yamada et al. 1990) and vertical thickness of at least 1.5 km based on borehole investigation. The Toki granite intruded into Jurassic sedimentary rocks (the Kamiasou Unit) of the Mino Terrane (Sano et al. 1992) and into the Nohi Rhyolite (85±5 Ma of allanite CHIME; Suzuki et al. 1998) (Fig. 2A). The Toki granite is surrounded by the sedimentary rocks of the Mino Terrane on the north and west, the Sumikawa granite on the south and the Nohi Rhyolite on the east (Yamashita et al. 1988). The intrusive contacts between the Toki granite and the sedimentary rocks of the Mino Terrane are sharp and observed at an outcrop (N69$^o$W 65$^o$S) about 1 km north of the study area (Asia Air Survey 1997) and also in a borehole DH-6 (N38$^o$W 44$^o$E at the elevation of 52.3 m). The pelitic and psammitic rocks of the Mino Terrane were metamorphosed to hornfels by the Toki granitic magma (Yamashita et al. 1988). The Toki granite is overlain unconformably by the Miocene Mizunami Group and the Pliocene Seto Group (Itoigawa 1974 and 1980). The Toki granite and the Mizunami Group are cut by the Tsukiyoshi fault, a reverse, dip-slip fault with an approximate N80$^o$W strike and 65-75$^o$ S dip (Yamashita et al. 1988; Ota et al. 1999). The Tsukiyoshi fault has been active intermittently since its formation in the Miocene up to the formation of Pliocene Seto Group (Fujii 2000).

The Toki granite is characterized by systematic spatial changes in rock facies (mode and mineral assemblage) and corresponding change in bulk chemical compositions, and is interpreted to be a zoned pluton (Yuguchi et al. 2010). The rock facies grades from muscovite – biotite granite (MBG) at the margin, through hornblende – biotite granite (HBG) to biotite granite (BG) in the interior (Fig. 2B). The boundaries of three rock facies are defined by appearance (MBG / HBG) and disappearance (HBG / BG) of hornblende without accompanying chilled margin. The systematic change in the Alumina Saturation Index (ASI) values (mol. $Al_2O_3$ / ($CaO$ + $Na_2O$ + $K_2O$) ) from the MBG through HBG to BG, corresponds to a systematic variation in the bulk chemistry from peraluminous at the margin to metaluminous in the interior. The $Fe^{3+}$ / $Fe^{2+}$ ratios gradually increase from MBG through HBG to BG, corresponding to a systematic change from ilmenite-series at the margin to magnetite-series in the interior (Yuguchi et al. 2010). This study employed hornblende, biotite and zircon for the thermochronometry. Hornblende only occurs in the HBG, whereas biotite and zircon commonly occur throughout the Toki granite.

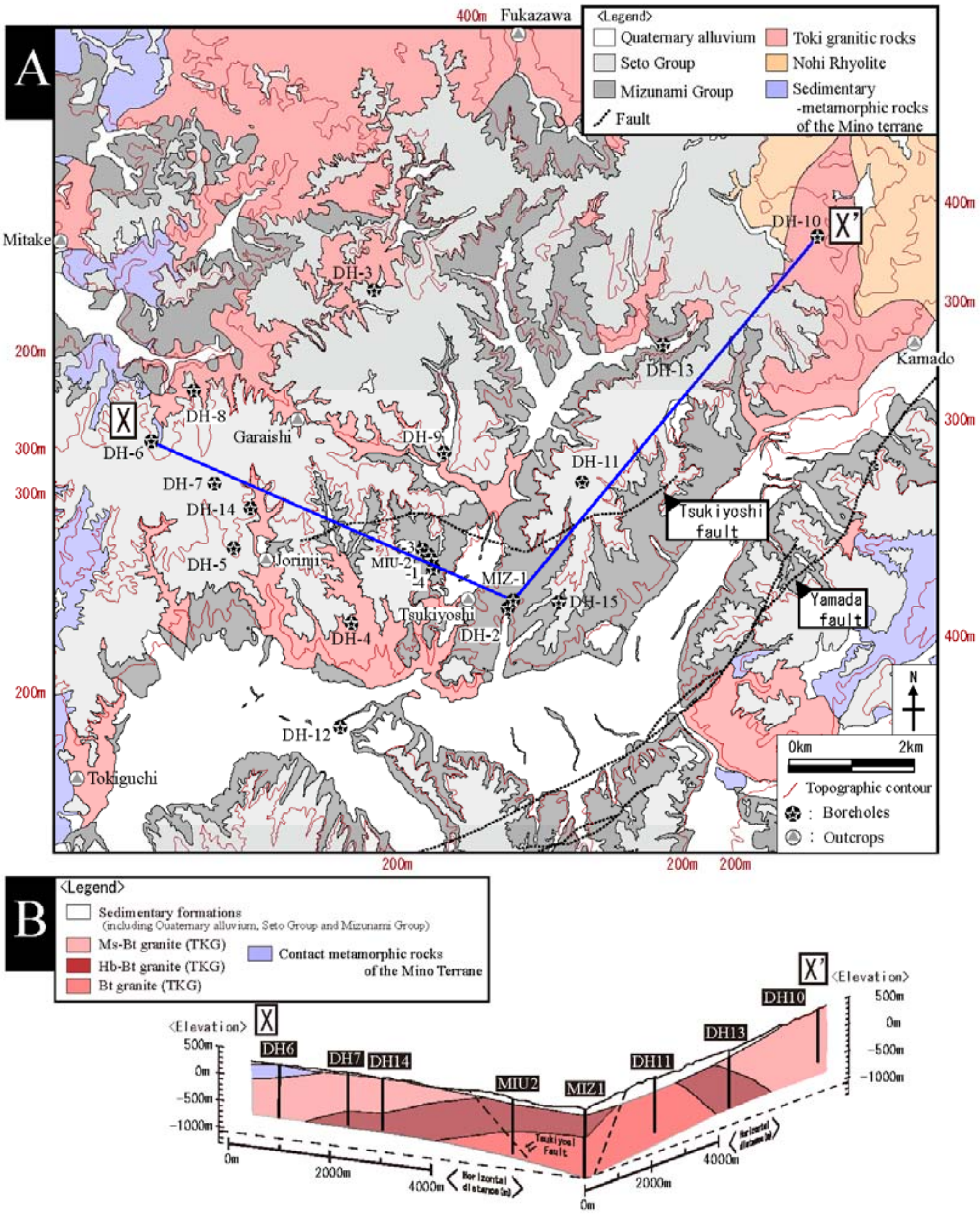


**Fig. 2** The Toki granitic pluton. (A) Geological map of the Tono district showing the Toki granite, after Itoigawa (1980), and borehole and outcrop sites in this study. The topographic contour inside the Tono district is based on Geographical Survey Institute, 1 : 25,000 topographic maps entitled Ontake, Takenami, Toki, and Mizunami. (B) Rock facies cross-section for the Toki granite along the line from X to X' in the topography map (Fig. 2A); Ms-Bt granite, Muscovite - biotite granite; Hb-Bt granite, hornblende - biotite granite; Bt granite, biotite granite (Yuguchi et al., 2010).

## Samples and analytical procedures

Samples used for this study were collected from 11 boreholes and seven outcrops (Fig. 2A) in order to examine the spatial variation in mineral ages in the cooling magma chamber. Hornblende, biotite and zircon were separated from rock samples by a combination of grain size separation, magnetic separation using a Franz Isodynamic Separator and density separation using conventional heavy liquid. Their representative compositions are listed in Table 1. Two data are obtained for hornblende K-Ar age, 33 data for biotite K-Ar age, and 44 data for zircon fission-track age (Table 2-4).

The potassium and argon analyses were carried out at the Hiruzen Institute for Geology and Chronology Co. Ltd., Geospace Science Co. Ltd. and Allegheny Technologies Japan Co. Ltd. Radiogenic argon concentrations were analyzed with an isotope dilution mass spectrometer (Kratos MS-10S and AEI MS-10) following the technique of Dalrymple and Lanphere (1969). Potassium was determined with a flame emission spectrophotometry utilizing an internal standard. The isotopic ages of the samples were calculated using the standard K-Ar age equation (Dalrymple and Lanphere 1969; Dalrymple et al. 1999) with $\lambda_\varepsilon = 0.581 \times 10^{-10}$ / yr, $\lambda_\beta = 4.962 \times 10^{-10}$ / yr and $^{40}K$ / K = 0.0001167 of Steiger and Jäger (1977). The analytical uncertainties associated with the age determination were calculated using the method of Cox and Dalrymple (1967). K-Ar closure temperatures in this study are based on Dodson and McClelland-Brown (1985) as follows: 510±25 °C for hornblende, and 300±50 °C for biotite.

Fission-track dating was carried out at Kyoto Fission-Track Co. Ltd., using zeta calibration method based on recommendation by the I.U.G.S. Subcommission on Geochronology (Hurford 1900a and 1900b). The density of spontaneous fission-tracks generated by $^{238}U$ decay in a mineral is proportional to the age and the $^{238}U$ content of the sample. The fission track age are obtained by the following

$$T = \frac{1}{\lambda_D} \ln\left(1 + \lambda_D \cdot g \cdot \zeta \cdot \frac{\rho_s}{\rho_i} \cdot \rho_d\right)$$

where $T$ = age, $\lambda_D$ = total decay constant of $^{238}U$, $g$ = geometry factor depending on detector type (Gleadow and Lovering 1977), $\zeta$ = zeta calibration factor, $\rho_s / \rho_i$ = spontaneous / induced fission track density ratio in the sample, and $\rho_d$ = density of induced fission track measured on the detector place in intimate contact to the glass monitor. Zircon samples were analyzed by the external detector method (ED1, internal mineral surface) using the geometry factor of 0.5 (Gleadow 1981). Zircons were etched in a NaOH and KOH eutectic mixture (Gleadow et al. 1976). Thermal irradiations of samples were carried out in the Rotary Speciment Rack of the TRIGA MARK II reactor at Rikkyo University and in the PN site of the JRR-4 reactor of JAEA. Fission-track ages were determined based on the zeta-calibration approach described by Hurford and Green (1983). The total decay constant of $^{238}U$ is $\lambda_D = 1.55125 \times 10^{-10}$ / yr (Steiger and Jäger 1977). Zeta calibration factors of zircon for ED1 are $\zeta_{ED1}$ = 352±3 (Danhara and Iwano 1983) for Rikkyo University reactor and $\zeta_{ED1}$ = 380±3 (Danhara et al. 2003) for JRR-4 reactor. The errors in zeta values are given to one sigma. Closure temperature for zircon fission-track dating is 240±50 °C based on Dodson and McClelland-Brown (1985).

Characterization of zircon fission-track length measurements was also carried out for nine samples to test possible rejuvenation by massive reheating during the cooling process, which were collected from three boreholes of DH-2, 10 and MIZ-1. Annealing will shorten the fission-track length, thus yielding a decrease in fission-track density. Track length measurement (track number, mean, maximum and minimum length, standard deviation and standard error) gives quantification of the shortening and distribution shift in track length, based on comparison with standard fission-track length sample (Fish Canyon Tuff: reheating-free sample).

**Table 1** Representative analyses of hornblende, biotite and zircon from the Toki granite.

| Mineral | Hb | Hb | Bt | Bt | Zr | Zr |
|---|---|---|---|---|---|---|
| Sample No. | DH13-15 | DH13-15 | MIU2-34 | MIU2-34 | MIU2-13 | MIZ1-23 |
| Elevation | -216.00m | -216.00m | -496.72m | -496.72m | -85.72m | -1010.29m |
| Location | 03-core | 03-rim | 04-core | 04-rim | 02-core | 03-core |
| (wt%) | | | | | | |
| **$SiO_2$** | 39.16 | 40.01 | 33.90 | 33.97 | 32.70 | 31.76 |
| **$TiO_2$** | 0.61 | 1.11 | 3.89 | 3.20 | - | - |
| **$Al_2O_3$** | 9.91 | 9.20 | 14.65 | 14.66 | - | - |
| **FeO** | 27.69 | 28.03 | 29.20 | 29.01 | - | - |
| **MnO** | 1.90 | 1.77 | 1.04 | 1.01 | - | - |
| **MgO** | 2.83 | 3.04 | 3.86 | 3.71 | - | - |
| **CaO** | 10.31 | 10.30 | - | - | - | - |
| **$Na_2O$** | 1.95 | 1.90 | 0.42 | 0.45 | - | - |
| **$K_2O$** | 1.15 | 0.96 | 9.63 | 10.11 | - | - |
| **$ZrO_2$** | - | - | - | - | 64.40 | 58.04 |
| **$HfO_2$** | - | - | - | - | 1.32 | 2.21 |
| **$P_2O_5$** | - | - | - | - | - | 1.91 |
| **$ThO_2$** | - | - | - | - | - | 2.07 |
| **$UO_3$** | - | - | - | - | 0.87 | 2.53 |
| total | 95.51 | 96.32 | 96.59 | 96.12 | 99.29 | 98.52 |
| (atm) | | | | | | |
| **O** | 23 | 23 | 22 | 22 | 4 | 4 |
| **Si** | 6.46 | 6.53 | 5.44 | 5.49 | 1.00 | 0.99 |
| **Ti** | 0.08 | 0.14 | 0.47 | 0.39 | - | - |
| **Al** | 1.93 | 1.77 | 2.77 | 2.79 | - | - |
| **Fe** | 3.82 | 3.83 | 3.92 | 3.92 | - | - |
| **Mn** | 0.27 | 0.24 | 0.14 | 0.14 | - | - |
| **Mg** | 0.70 | 0.74 | 0.92 | 0.89 | - | - |
| **Ca** | 1.82 | 1.80 | - | - | - | - |
| **Na** | 0.62 | 0.60 | 0.13 | 0.14 | - | - |
| **K** | 0.24 | 0.20 | 1.97 | 2.08 | - | - |
| **Zr** | - | - | - | - | 0.97 | 0.88 |
| **Hf** | - | - | - | - | 0.01 | 0.02 |
| **P** | - | - | - | - | - | 0.05 |
| **Th** | - | - | - | - | - | 0.01 |
| **U** | - | - | - | - | 0.01 | 0.02 |
| total | 15.94 | 15.85 | 15.76 | 15.84 | 1.99 | 1.98 |

**Table 2** Hornblende K-Ar dating results from the Toki Granite

| Sample description | | | *Rock facies | Sample location and elevation | | | K | Rad. $^{40}$Ar | | **Age (Ma)** | ± | **1σ** |
|---|---|---|---|---|---|---|---|---|---|---|---|---|
| Borehole (B) / Outcrop (O) | | Sample name | | X (northing) | Y (easting) | Elevation (m) | (wt%) | (scc / gm × $10^{-5}$) | (wt%) | | | |
| **O** | Mitake | KA-5Hbg | MBG | -63940.0 | 350.0 | 290.0 | 1.25 | 0.37 | 73.6 | 74.6 | ± | 3.7 |
| **O** | Mitake | KA-5Hby | MBG | -63940.0 | 350.0 | 290.0 | 0.82 | 0.24 | 67.5 | 73.9 | ± | 3.7 |

*Rock facies of the Toki granite includes muscovite-biotite granite (MBG), hornblende-biotite granite (HBG) and biotite granite (BG).

**Table 3** Biotite K-Ar dating results from the Toki Granite

| Sample description | | | *Rock facies | Sample location and elevation | | | K | Rad. $^{40}$Ar | | **Age (Ma)** | ± | **1σ** |
|---|---|---|---|---|---|---|---|---|---|---|---|---|
| Borehole (B) / Outcrop (O) | | Sample name | | X (northing) | Y (easting) | Elevation (m) | (wt%) | (scc / gm × $10^{-5}$) | (wt%) | | | |
| **B** | DH-2 | DH02RA01 | HBG | -69125.0 | 6437.4 | -185.0 | 7.18 | 2.06 | 96.2 | 72.3 | ± | 1.8 |
| **B** | DH-2 | DH02RA03 | BG | -69125.0 | 6437.4 | -302.1 | 7.10 | 2.06 | 94.7 | 73.0 | ± | 1.8 |
| **B** | DH-3 | DH3-1 | MBG | -64489.2 | 4416.3 | 77.0 | 6.24 | 1.86 | 92.2 | 75.0 | ± | 1.9 |
| **B** | DH-3 | DH3-2 | MBG | -64489.2 | 4416.3 | -479.7 | 5.80 | 1.68 | 89.2 | 73.1 | ± | 1.8 |
| **B** | DH-8 | FT-5 | MBG | -66002.9 | 1871.9 | 47.3 | 5.87 | 1.69 | 98.2 | 72.9 | ± | 1.8 |
| **B** | DH-8 | FT-6 | MBG | -66002.9 | 1871.9 | -88.2 | 6.57 | 1.87 | 96.8 | 71.8 | ± | 1.6 |
| **B** | DH-8 | FT-7 | MBG | -66002.9 | 1871.9 | -439.6 | 6.37 | 1.84 | 98.4 | 73.0 | ± | 1.6 |
| **B** | DH-8 | FT-8a | MBG | -66002.9 | 1871.9 | -610.7 | 6.46 | 1.86 | 98.4 | 72.9 | ± | 1.7 |
| **B** | DH-8 | FT-8b | MBG | -66002.9 | 1871.9 | -739.7 | 6.44 | 1.86 | 98.4 | 72.9 | ± | 1.7 |
| **B** | DH-10 | DH10 | MBG | -63745.2 | 10945.7 | 196.2 | 6.95 | 2.04 | 95.3 | 74.0 | ± | 1.8 |
| **B** | DH-10 | DH10RA | MBG | -63745.2 | 10945.7 | -256.2 | 6.86 | 1.96 | 94.7 | 72.0 | ± | 1.8 |
| **B** | DH-11 | DH11-1 | BG | -67285.4 | 7560.5 | -116.7 | 2.62 | 0.69 | 88.6 | 66.3 | ± | 1.7 |
| **B** | DH-11 | DH11-2 | BG | -67285.4 | 7560.5 | -411.9 | 6.35 | 1.82 | 94.4 | 72.3 | ± | 1.8 |
| **B** | DH-12 | DH12 | MBG | -70695.4 | 3935.0 | -246.7 | 6.98 | 2.07 | 95.6 | 74.5 | ± | 1.9 |
| **B** | DH-13 | DH13 | HBG | -65324.7 | 8625.8 | -77.0 | 6.22 | 1.83 | 95.3 | 73.9 | ± | 1.8 |
| **B** | MIU-1 | KA-1bi | HBG | -68280.3 | 5217.4 | 108.6 | 4.64 | 1.37 | 90.7 | 74.1 | ± | 3.7 |
| **B** | MIU-1 | KA-2Bi | HBG | -68280.3 | 5217.4 | -261.9 | 6.74 | 2.02 | 95.3 | 75.0 | ± | 3.8 |
| **B** | MIU-1 | KA-3Bi | BG | -68280.3 | 5217.4 | -360.9 | 6.61 | 1.97 | 89.6 | 74.9 | ± | 3.7 |
| **B** | MIU-1 | KA-4Bi | BG | -68280.3 | 5217.4 | -520.1 | 6.28 | 1.84 | 90.6 | 73.6 | ± | 3.7 |
| **B** | MIU-4 | MIU-4FT2-02 | HBG | -68292.5 | 5353.0 | -98.5 | 2.27 | 0.54 | 51.9 | 60.1 | ± | 1.5 |
| **B** | MIU-4 | MIU-4FT3-02 | HBG | -68268.7 | 5376.7 | -176.2 | 1.34 | 0.33 | 73.0 | 63.1 | ± | 1.6 |
| **B** | MIU-4 | MIU-4FT5-02 | HBG | -68237.2 | 5408.2 | -279.3 | 1.20 | 0.28 | 60.8 | 59.7 | ± | 1.5 |
| **B** | MIU-4 | MIU-4FT6-02 | HBG | -68243.9 | 5401.5 | -257.2 | 3.24 | 0.79 | 88.5 | 61.4 | ± | 1.5 |
| **B** | MIZ-1 | MIZ01RA01 | HBG | -68867.7 | 6503.7 | 95.7 | 6.97 | 1.98 | 95.8 | 71.5 | ± | 1.8 |
| **B** | MIZ-1 | MIZ01RA03 | HBG | -68867.7 | 6503.7 | 23.7 | 6.74 | 1.96 | 94.6 | 73.1 | ± | 1.8 |
| **B** | MIZ-1 | MIZ01RA05 | HBG | -68825.1 | 6546.3 | -69.9 | 7.03 | 2.01 | 95.5 | 72.1 | ± | 1.8 |
| **O** | Mitake | KA-5Bi | MBG | -63940.0 | 350.0 | 290.0 | 7.06 | 2.20 | 91.2 | 78.5 | ± | 3.9 |
| **O** | Fukazawa | KA-6Bi | MBG | -60947.9 | 6706.5 | 290.0 | 7.02 | 2.16 | 91.3 | 77.3 | ± | 3.9 |
| **O** | Kamado | KA-7Bi | MBG | -65670.0 | 12380.0 | 268.0 | 7.09 | 2.01 | 89.8 | 71.4 | ± | 3.6 |
| **O** | Garaishi | KA-8Bi | MBG | -66730.0 | 3535.0 | 330.0 | 6.90 | 2.11 | 91.1 | 76.9 | ± | 3.8 |
| **O** | Tsukiyoshi | KA-9Bi | HBG | -69385.0 | 5885.0 | 179.0 | 5.96 | 1.78 | 93.2 | 75.2 | ± | 3.8 |
| **O** | Jorinji | KA-10Bi | MBG | -68827.5 | 3162.5 | 230.0 | 6.49 | 1.96 | 82.0 | 75.9 | ± | 3.8 |
| **O** | Tokiguchi | KA-11Bi | MBG | -72025.0 | 390.0 | 130.0 | 6.24 | 1.94 | 91.6 | 78.3 | ± | 3.9 |

*Rock facies of the Toki granite includes muscovite-biotite granite (MBG), hornblende-biotite granite (HBG) and biotite granite (BG).

**Thermochronology: K-Ar dating and fission-track dating**

The results of the K-Ar dating and fission-track dating for minerals are listed in Table 2-4. Hornblende K-Ar ages are about 74.3±3.7 Ma (Fig. 3). Biotite K-Ar ages range from 78.5±3.9 to 59.7±1.5 Ma, with a distribution of approximately 20 Ma (Fig. 3). The zircon fission-track ages range from 75.6±3.3 to 52.8±2.6 Ma, with a scatter of 23 Ma (Fig. 3). Characterization of zircon fission-track length measurements gives almost same results for nine samples, which show normal frequency distribution ranging from 5 to 12 μm (Table 5 and Fig. 4). Mean fission-track length clusters range from 10 to 11 μm with a single frequency peak (Fig. 4). This result indicates that the ages do not represent rejuvenation by massive reheating during the cooling process.

The mineral age will represent the time at which mineral cooled down to the closure temperature, if the Toki granitic pluton was emplaced as a one pulse or if the emplacement duration is much shorter than the cooling duration in the case of multiple pulse intrusion. The Toki granite shows three rock facies with variations of mineral assemblage among them, without accompanying chilled margin. They have neither mingling texture nor non-equilibrium mineral assemblage. Plagioclase has no dusty zone, indicating the absence of magma mixing. These lines of evidence suggest the single pulse intrusion of the Toki granite in terms of petrography. The dating of the Toki granite using monazite CHIME and whole-rock Rb-Sr method gives 72.3±3.9 Ma (Suzuki and Adachi 1998) and 68.3±1.8 Ma (Shibata and Ishihara 1979), respectively, which will represent the emplacement age (Albarède 2003). The whole-rock Rb-Sr age determined by 14 isotopic data collected through three rock facies (4 samples of MBG, 5 samples of HBG and 5 samples of BG) is 71.04 ± 1.44 Ma (Yuguchi et al. in perp.A), which is consistent with the result of Shibata and Ishihara (1979). Hornblende K-Ar age represents a timing with closure temperature of 510±25 °C, which are about 74.3±3.7 Ma (Table 2). These dating results cluster in a range of about 4 million years, which implies that the total emplacement duration is either shorter than, or equal to, 4 million years. The duration from the hornblende K-Ar age to the youngest age in zircon fission-track dating is about 22 million years (Fig. 3), which represents cooling duration from 510±25 °C to 240±50 °C. The duration from the hornblende K-Ar age to the youngest age in apatite fission-track is about 42 million years (Yuguchi et al. in perp.B), which corresponds to the cooling duration from 510±25 °C to 120±20 °C. These petrographical observations and chronological results indicate that the total emplacement duration of the Toki granite is much shorter than the total cooling duration. Therefore, since the age of a mineral represents the age when the Toki granite cooled down to the closure temperature of the mineral, the older age represents more rapid cooling than the younger age. The spatial cooling history inside the granite can be clarified by a combination of biotite K-Ar and zircon fission-track ages (Table 3 and 4). Hornblende K-Ar age was excluded from the consideration, because of their limited distribution to only one borehole (n=2) (Table 2). The results for the biotite K-Ar and zircon fission-track dating exhibit distribution in excess of the two-sigma level for each mineral age, indicating differences in cooling rate inside the granite pluton (Fig. 3). Age data collected from borehole and outcrop samples were interpolated and converted to 3D data for visualization using the software Rock Works 14®.

MBG possesses biotite K-Ar age ranging from 78.5±3.9 to 71.4±3.9 Ma (N=16) and zircon fission-track age from 75.6±3.3 to 52.8±2.6 Ma (N=20) (Table 3 and 4). HBG shows the biotite age varying from 75.2±3.8 to 59.7±1.5 Ma (N=12) and the zircon age from 64.3±3.2 to 54.6±2.4 Ma (N=19). BG presents the biotite age ranging from 74.9±3.7 to 66.3±1.7 Ma (N=5) and the zircon age from 64.1±2.7 to 57.2±2.3 Ma (N=5). The oldest ages in both datings are recognized in MBG. Figure 5A and B show the contoured spatial distribution of biotite K-Ar ages and zircon fission-track ages respectively, on fence and block diagrams. Vertical elevations given in the text are with respect to the mean sea level, not the depth from the topographic surface, i.e. positive/negative value denotes upper/lower region with respect to the mean sea level, respectively. This allows a comparison of the age data in terms of the vertical coordinate (elevation). The distribution of biotite K-Ar ages has the same tendency as that of the zircon fission-track ages. The youngest ages (warm colors) are found in the deeper regions of the MIU sites and the oldest ages, (cold colors) are distributed at the northwest upper margin of the pluton (Fig. 5A and B). The biotite K-Ar dating gives ages of 61.4±1.5 Ma in the central deeper region (-257.2 m elevation of MIU-4) and of 72.9±1.8 Ma at the northwest upper margin (47.3 m elevation of DH-8) (Table 3). Table 4 shows the zircon fission-track ages of 58.9±2.7 Ma in the central deeper region (-520.1 m elevation of MIU-1) and of 68.7±2.8 Ma at the northwest upper margin (50.8 m elevation of DH-6). The zircon fission-track age indicates that the Toki granite effectively cooled from the roof and the northwest margin from 75 to 65 Ma (Fig. 5B). Then the northeast margin cooled down in the period from 65 to 61 Ma (Fig. 5B) followed by the southern and central regions (boreholes MIU-1 to -4) from 61 to 55 Ma (Fig. 5B). These data show that the cooling started from the roof and the northwest margin of the Toki granite, and then extended to the northeast and further to the central and southern regions.

**Table 4** Zircon fission-track dating results from the Toki Granite

| Sample description | | | *Rock facies | Location and elevation | | | N** | Spontaneous | | Induced | | $P(\chi^2)$ | Dosimeter | | r | U (ppm) | Age (Ma) | ± | 1σ |
|---|---|---|---|---|---|---|---|---|---|---|---|---|---|---|---|---|---|---|---|
| Borehole (B) / Outcrop (O) | | Sample name | | X (northing) | Y (easting) | Eleva-tion (m) | | $\rho_s$ ($10^{-6}$ cm$^{-2}$) | $N_s$ | $\rho_i$ ($10^{-6}$ cm$^{-2}$) | $N_i$ | | $\rho_d$ ($10^4$ cm$^{-2}$) | $N_d$ | | | | | |
| B | DH-2 | RA01 | HBG | -69125.0 | 6437.4 | -185.0 | 30 | 9.15 | 3814 | 2.20 | 918 | 0 | 8.138 | 4167 | 0.489 | 260 | 63.9 | ± | 2.6 |
| B | DH-2 | RA03 | BG | -69125.0 | 6437.4 | -302.1 | 30 | 8.95 | 3402 | 2.41 | 917 | 10 | 8.153 | 4174 | 0.644 | 280 | 57.2 | ± | 2.3 |
| B | DH-3 | DH3-1 | MBG | -64489.2 | 4416.3 | 77.0 | 30 | 7.51 | 4764 | 1.95 | 1239 | 70 | 8.698 | 4453 | 0.779 | 210 | 63.2 | ± | 2.3 |
| B | DH-3 | DH3-2 | MBG | -64489.2 | 4416.3 | -479.7 | 30 | 8.12 | 4612 | 2.00 | 1134 | 0 | 8.715 | 4462 | 0.698 | 220 | 67.0 | ± | 2.5 |
| B | DH-6 | FT-5 | MBG | -66630.9 | 978.7 | 13.3 | 30 | 8.78 | 3584 | 1.98 | 807 | 0 | 8.370 | 2571 | 0.332 | 190 | 65.1 | ± | 2.9 |
| B | DH-6 | FT-6 | MBG | -66630.9 | 978.7 | -126.9 | 30 | 8.46 | 3731 | 1.87 | 823 | 0 | 8.373 | 2572 | 0.525 | 180 | 66.5 | ± | 2.9 |
| B | DH-6 | FT-7 | MBG | -66630.9 | 978.7 | -473.6 | 20 | 9.63 | 2657 | 2.25 | 621 | 3 | 8.377 | 2573 | 0.611 | 220 | 62.8 | ± | 3.1 |
| B | DH-6 | FT-8 | MBG | -66630.9 | 978.7 | 50.8 | 30 | 11.10 | 4826 | 2.37 | 1030 | 1 | 8.380 | 2574 | 0.386 | 230 | 68.7 | ± | 2.8 |
| B | DH-8 | FT-5 | MBG | -66002.9 | 1871.9 | 47.3 | 30 | 9.23 | 4599 | 1.71 | 854 | 0 | 8.025 | 2465 | 0.407 | 170 | 75.6 | ± | 3.3 |
| B | DH-8 | FT-6 | MBG | -66002.9 | 1871.9 | -88.2 | 30 | 9.25 | 4348 | 1.90 | 891 | 3 | 8.027 | 2466 | 0.479 | 190 | 68.6 | ± | 2.9 |
| B | DH-8 | FT-7 | MBG | -66002.9 | 1871.9 | -439.6 | 30 | 10.70 | 5519 | 2.10 | 1082 | 0 | 8.029 | 2467 | 0.585 | 210 | 71.7 | ± | 2.9 |
| B | DH-8 | FT-8a | MBG | -66002.9 | 1871.9 | -610.7 | 30 | 8.80 | 5115 | 1.77 | 1031 | 0 | 8.031 | 2467 | 0.786 | 180 | 69.7 | ± | 2.8 |
| B | DH-8 | FT-8b | MBG | -66002.9 | 1871.9 | -739.7 | 30 | 8.64 | 5799 | 1.77 | 1188 | 17 | 8.033 | 2468 | 0.735 | 180 | 68.6 | ± | 2.7 |
| B | DH-10 | DH10 | MBG | -63745.2 | 10945.7 | 196.2 | 30 | 7.31 | 4482 | 1.62 | 996 | 23 | 8.612 | 4409 | 0.664 | 180 | 73.2 | ± | 2.9 |
| B | DH-10 | DH10RA | MBG | -63745.2 | 10945.7 | -256.2 | 30 | 6.08 | 5401 | 1.34 | 1191 | 14 | 8.131 | 4163 | 0.663 | 160 | 69.7 | ± | 2.5 |
| B | DH-11 | DH11-1 | BG | -67285.4 | 7560.5 | -116.7 | 30 | 9.79 | 3662 | 2.58 | 964 | 11 | 8.629 | 4418 | 0.526 | 280 | 62.0 | ± | 2.5 |
| B | DH-11 | DH11-2 | BG | -67285.4 | 7560.5 | -411.9 | 30 | 9.85 | 3221 | 2.51 | 822 | 5 | 8.646 | 4427 | 0.675 | 270 | 64.1 | ± | 2.7 |
| B | DH-12 | DH12 | MBG | -70695.4 | 3935.0 | -246.7 | 30 | 9.65 | 4158 | 2.70 | 1163 | 0 | 8.663 | 4436 | 0.647 | 290 | 58.6 | ± | 2.2 |
| B | DH-13 | DH13 | HBG | -65324.7 | 8625.8 | -77.0 | 30 | 12.00 | 3696 | 3.31 | 1019 | 0 | 8.680 | 4444 | 0.636 | 360 | 59.5 | ± | 2.3 |
| B | MIU-1 | FT-1 | HBG | -68280.3 | 5217.4 | 108.6 | 30 | 11.00 | 3828 | 2.59 | 902 | 9 | 8.356 | 2567 | 0.657 | 250 | 62.1 | ± | 2.7 |
| B | MIU-1 | FT-2 | HBG | -68280.3 | 5217.4 | -261.9 | 30 | 10.80 | 4080 | 2.48 | 939 | 0 | 8.359 | 2568 | 0.507 | 240 | 63.6 | ± | 2.7 |
| B | MIU-1 | FT-3 | BG | -68280.3 | 5217.4 | -360.9 | 30 | 9.50 | 4313 | 2.35 | 1065 | 1 | 8.363 | 2569 | 0.410 | 230 | 59.3 | ± | 2.4 |
| B | MIU-1 | FT-4 | BG | -68280.3 | 5217.4 | -520.1 | 30 | 10.20 | 2989 | 2.55 | 744 | 0 | 8.366 | 2570 | 0.414 | 240 | 58.9 | ± | 2.7 |
| B | MIU-4 | FT2-02 | HBG | -68292.4 | 5353.0 | -98.6 | 30 | 10.40 | 4864 | 2.71 | 1265 | 1 | 8.456 | 2165 | 0.645 | 260 | 57.0 | ± | 2.2 |
| B | MIU-4 | FT3-03 | HBG | -68268.6 | 5376.8 | -176.5 | 30 | 9.55 | 4786 | 2.52 | 1263 | 10 | 8.562 | 2192 | 0.555 | 240 | 56.9 | ± | 2.2 |
| B | MIU-4 | FT6-02 | HBG | -68243.9 | 5401.5 | -257.2 | 28 | 11.20 | 3415 | 2.85 | 873 | 1 | 8.601 | 2202 | 0.355 | 270 | 58.9 | ± | 2.6 |
| B | MIU-4 | FT4-02 | HBG | -68241.2 | 5404.2 | -266.2 | 30 | 9.80 | 3519 | 2.47 | 887 | 0 | 8.496 | 2175 | 0.599 | 230 | 59.1 | ± | 2.6 |
| B | MIU-4 | FT5-02 | HBG | -68237.2 | 5408.2 | -279.3 | 30 | 9.89 | 2808 | 2.68 | 761 | 2 | 8.522 | 2182 | 0.720 | 250 | 55.1 | ± | 2.6 |
| B | MIU-4 | FT7 | HBG | -68271.4 | 5374.0 | -167.3 | 30 | 14.00 | 4953 | 3.45 | 1223 | 2 | 8.617 | 2206 | 0.422 | 360 | 61.1 | ± | 2.4 |
| B | MIU-4 | FT8 | HBG | -68259.1 | 5386.3 | -207.7 | 30 | 12.60 | 5409 | 3.43 | 1469 | 5 | 8.619 | 2206 | 0.376 | 360 | 55.6 | ± | 2.1 |
| B | MIU-4 | FT9 | HBG | -68231.9 | 5413.5 | -296.5 | 30 | 11.70 | 3453 | 3.25 | 956 | 0 | 8.620 | 2207 | 0.551 | 340 | 54.6 | ± | 2.4 |
| B | MIZ-1 | RA01 | HBG | -68867.7 | 6503.7 | 98.4 | 30 | 9.91 | 4628 | 2.54 | 1184 | 0 | 8.043 | 4118 | 0.667 | 300 | 59.5 | ± | 2.2 |
| B | MIZ-1 | RA03 | HBG | -68867.7 | 6503.7 | 28.1 | 30 | 8.62 | 4381 | 2.10 | 1068 | 9 | 8.057 | 4125 | 0.774 | 250 | 62.5 | ± | 2.4 |
| B | MIZ-1 | RA05 | HBG | -68825.1 | 6546.3 | -69.9 | 30 | 9.09 | 4563 | 2.46 | 1237 | 0 | 8.072 | 4133 | 0.583 | 290 | 56.3 | ± | 2.1 |
| B | MIZ-1 | RA07 | HBG | -68867.7 | 6503.7 | -6.1 | 30 | 10.80 | 3981 | 2.90 | 1066 | 4 | 8.087 | 4140 | 0.739 | 340 | 57.1 | ± | 2.2 |
| B | MIZ-1 | RA08 | HBG | -68867.7 | 6503.7 | 16.5 | 30 | 10.40 | 3848 | 2.78 | 1026 | 34 | 8.102 | 4148 | 0.521 | 320 | 57.5 | ± | 2.3 |
| B | MIZ-1 | RA09 | HBG | -68867.7 | 6503.7 | 16.5 | 29 | 10.40 | 2404 | 2.47 | 574 | 47 | 8.116 | 4156 | 0.696 | 290 | 64.3 | ± | 3.2 |
| O | Mitake | FT-9 | MBG | -63940.0 | 350.0 | 290.0 | 30 | 6.48 | 5218 | 1.52 | 1221 | 0 | 8.352 | 2566 | 0.674 | 150 | 62.5 | ± | 2.4 |
| O | Fukazawa | FT-10 | MBG | -60947.9 | 6706.5 | 290.0 | 30 | 7.71 | 3578 | 1.79 | 829 | 0 | 8.342 | 2563 | 0.591 | 170 | 63.1 | ± | 2.8 |
| O | Kamado | FT-11 | MBG | -65670.0 | 12380.0 | 268.0 | 21 | 13.60 | 2337 | 3.77 | 648 | 3 | 8.245 | 2564 | 0.770 | 360 | 52.8 | ± | 2.6 |
| O | Garaishi | FT-12 | MBG | -66730.0 | 3535.0 | 330.0 | 30 | 8.19 | 4600 | 1.92 | 1081 | 0 | 8.384 | 2576 | 0.628 | 180 | 62.5 | ± | 2.5 |
| O | Tsukiyosh | FT-13 | HBG | -69385.0 | 5885.0 | 179.0 | 30 | 8.63 | 3799 | 2.25 | 992 | 2 | 8.387 | 2577 | 0.588 | 220 | 56.3 | ± | 2.3 |
| O | Jorinji | FT-14 | MBG | -68827.5 | 3162.5 | 230.0 | 30 | 8.73 | 3371 | 1.93 | 745 | 0 | 8.338 | 2561 | 0.620 | 190 | 66.1 | ± | 3.0 |
| O | Tokiguch | FT-15 | MBG | -72025.0 | 390.0 | 130.0 | 30 | 7.67 | 4280 | 1.73 | 963 | 0 | 8.349 | 2565 | 0.564 | 170 | 65.0 | ± | 2.7 |

*Rock facies of the Toki granite includes muscovite-biotite granite (MBG), hornblende-biotite granite (HBG) and biotite granite (BG). Note: Analyses were obtained by the external detector method using internal mineral surfaces and a geometry factor of 0.5 (ED1: Gleadow, 1981). N** denotes the number of grains. $\rho_s$ is the spontaneous track density (tracks / cm$^2$) in the grain and Ns stands for the number of spontaneous tracks. $\rho_i$ and $N_i$ is the induced track density (tracks / cm$^2$) and number, respectively, in the external detector (tracks / cm$^2$). $\rho_d$ is the track density (tracks / cm$^2$) and $N_d$ stands for the number of tracks in the doisimeter glass. $P(x^2)$ is the probability of obtaining the $x^2$-value for n degrees of freedom. r is the correlation coefficient between $\rho_s$ and $\rho_i$. Details of experimental conditions and calibration factors are described by Iwano and Danhara (1997) and Danhara et al. (2003).

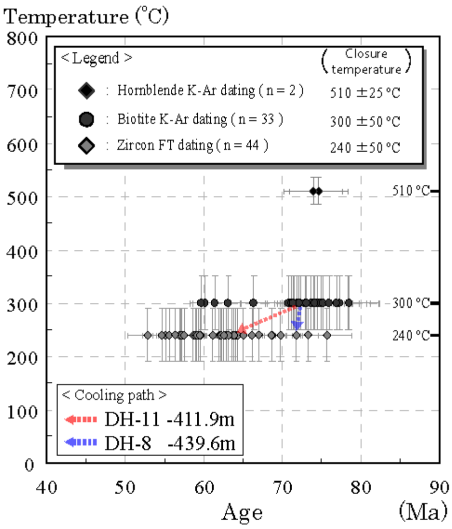


**Fig. 3** Age distribution against closure temperatures. Closure temperatures of the three minerals are from Dodson and McClelland-Brown (1985) and Hurford (1986): hornblende, K-Ar 510±25 °C; biotite, K-Ar 300±50 °C; zircon, Fission-track 240±50 °C. Red and blue dash arrows denote the sub-solidus temperature-time path of DH-11 -411.9 m elevation (central region of the granite body) and DH-8 -439.6 m elevation (northwest margin), respectively.

**Table 5** Characterization of zircon fission-track length measurements

| Sample description | | | Age (Ma) | ± | 1σ | Track number | Fission-track length | | | | |
|---|---|---|---|---|---|---|---|---|---|---|---|
| Borehole (B) / Standard (S) | | Sample name | | | | | Mean (μm) | Min. (μm) | Max. (μm) | Standard deviation | Standard error |
| B | DH-2 | RA01 | 63.9 | ± | 2.6 | 50 | 10.54 | 7.59 | 11.65 | 0.62 | 0.09 |
| B | DH-2 | RA03 | 57.2 | ± | 2.3 | 50 | 10.54 | 8.24 | 11.83 | 0.83 | 0.12 |
| B | DH-10 | DH10RA | 69.7 | ± | 2.5 | 50 | 10.43 | 5.12 | 11.83 | 1.16 | 0.16 |
| B | MIZ-1 | RA01 | 59.5 | ± | 2.2 | 50 | 10.27 | 5.30 | 11.89 | 1.14 | 0.16 |
| B | MIZ-1 | RA03 | 62.5 | ± | 2.4 | 50 | 10.47 | 8.35 | 11.88 | 0.66 | 0.09 |
| B | MIZ-1 | RA05 | 56.3 | ± | 2.1 | 50 | 10.56 | 6.88 | 11.97 | 0.88 | 0.12 |
| B | MIZ-1 | RA07 | 57.1 | ± | 2.2 | 50 | 10.40 | 6.34 | 11.96 | 0.88 | 0.12 |
| B | MIZ-1 | RA08 | 57.5 | ± | 2.3 | 50 | 10.06 | 5.68 | 11.66 | 1.32 | 0.19 |
| B | MIZ-1 | RA09 | 64.3 | ± | 3.2 | 50 | 10.26 | 7.58 | 11.86 | 0.91 | 0.13 |
| S | Fish Canyon Tuff | | | – | | 50 | 10.66 | 9.35 | 12.73 | 0.67 | 0.10 |

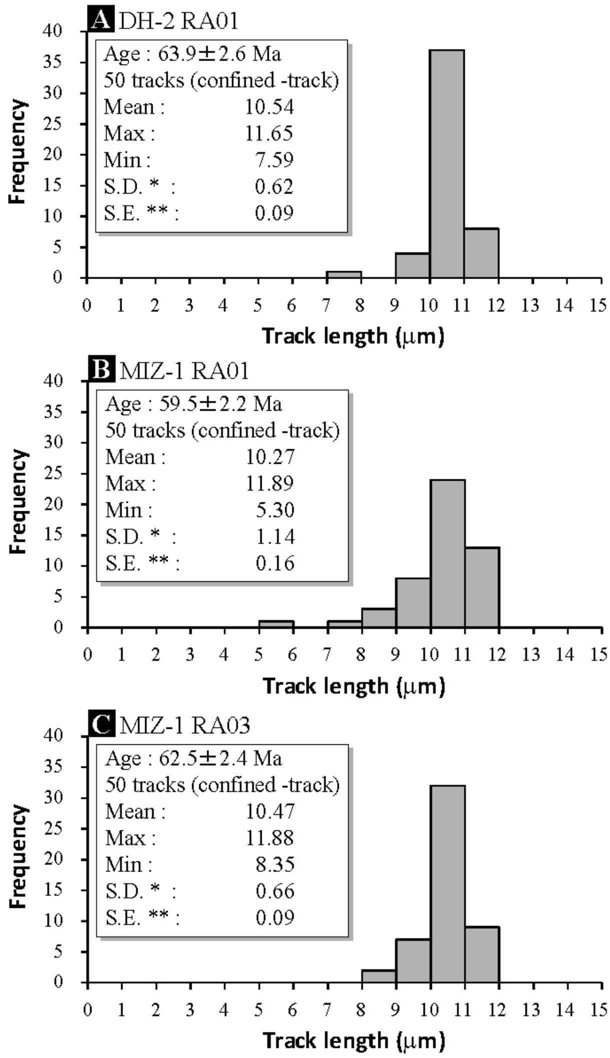


**Fig. 4** Frequency distribution of zircon fission-track length in three samples (A: DH-2 RA01, B: MIZ-1 RA01 and C: MIZ-1 RA03) collected from the Toki granite. (*S.D. ; standard deviation, **S.E. ; standard error)

## Discussion

Duration of cooling from biotite K-Ar closure temperature to zircon fission-track closure temperature

"Sub-solidus temperature-time path" at the particular position inside the Toki granite could be identified by comparing biotite K-Ar age and zircon fission-track age at the particular sample (Fig. 3). The gradient of temperature-time path depends on the position inside the granite, as the two representative cooling paths are schematically shown in Fig. 3: DH-11 (-411.9 m elevation at the central region of the granite body) and DH-8 (-439.6 m elevation at the northwest margin). Figure 6A shows a more detailed temperature-time relationship between biotite K-Ar and zircon fission-track ages in the two samples. The difference between the two ages at one particular position (or two positions within 5 m) inside the granite indicates the cooling duration in which the granite cooled from biotite K-Ar closure temperature ($300 \pm 50$ $^{o}$C) to zircon fission-track closure temperature ($240 \pm 50$ $^{o}$C). This cooling duration of the northwest margin of the body (1.3 million years of DH-8) is shorter than that of the central region (8.2 million years of DH-11) (Fig.6A). Figure 6B shows the contoured spatial distribution of the cooling duration between two closure temperatures on fence diagram, which was colored as a three-dimensional pattern using the software Rock Works 14® based on 33 data (Tables 3 and 4). The long duration (warm colors) are found at southern to central region, and the short duration (cold colors) are distributed at the northwest and northeast upper margin of the pluton. The cooling duration between two closure temperatures gives about 14.7 million years in the central deeper region (-520.1 m elevation of MIU-1) and of about 3.2 million years at the northwest upper margin (88.2 m elevation of DH-8). The distribution of cooling duration between two closure temperatures (Fig. 6B) has a pattern, consistent with that of cooling pattern based on "multi-sampling thermochronology" (Fig. 5A and B). Thus, the region with relatively early cooling (older ages) corresponds to that of the rapid rate of cooling from biotite K-Ar closure to zircon fission-track closure temperatures, and the region with relatively later cooling (younger ages) also corresponds to that of the slower cooling rate. Assuming simply that temperature difference between biotite K-Ar and zircon fission-track closure is 60 $^{o}$C, the cooling rate from 300 to 240 $^{o}$C at the central deeper region is about 4.1 $^{o}$C / m.y. (-520.1 m elevation of MIU-1), and that of northwest upper margin is 18.8 $^{o}$C / m.y. (88.2 m elevation of DH-8).

A factor controlling the cooling process

Figure 7 shows the contoured spatial distribution of the ASI values on the fence diagram based on 483 analyses of samples collected from boreholes in the Toki granite. Original data are taken from Yuguchi et al. (2010). The ASI values increase systematically from the roof downward. The minimum ASI value (in purple) occurs in the lower central region and larger values (warm colors) are distributed near the upper northwest margin (Fig. 7).

Yuguchi et al. (2010) discussed that the intrusion/emplacement process of the Toki granitic pluton probably includes assimilation of crustal country rocks into the granitic magma. The ASI values can be an index of the assimilation of the older sedimentary rock into the granitic magma (Pitcher 1997). Yuguchi et al. (2010) also described 1) the comparison of ASI between the Toki granite and the country sedimentary rocks of the Mino Terrane and 2) rare occurrence of the xenolith in the granite, which implies either that the xenolith was completely assimilated by the granitic magma or that the melt extracted from partially molten country rock was assimilated into the granitic magma. The country rock of the Toki granite is the Nohi Rhyolite on the east of the body and the sedimentary rocks of the Mino Terrane on the west. Assimilation of the sedimentary rocks of the Mino Terrane can yield the larger ASI than that of the Nohi Rhyolite. In fact, ASI value of the Nohi Rhyolite is almost equal to that of HBG and BG in the Toki granite (Yuguchi et al. 2010; Sonehara and Harayama 2007). Larger ASI values are distributed near the northwest margin in contact with the metasedimentary rocks (hornfels) of the Mino Terrane. Thus, geology around the Toki granite and ASI distribution inside the granite imply that the assimilation by the Toki granitic magma is operated during in-situ emplacement process, but not during magma ascent process before the emplacement.

Both biotite K-Ar dating and zircon fission-track dating show the same cooling pattern. The older age represents earlier and more rapid cooling, because mineral age is equivalent to the time at which the Toki granite cooled down to the closure temperature. Thus, the Toki granite effectively cooled down from the roof and also from the northwest margin at temperatures between 300±50 °C and 240±50 °C. There is a strong correlation between ASI (Fig. 7) and the cooling behavior of the pluton during this temperature stage (Fig. 5 and 6). Large ASI values correspond to earlier and more rapid cooling after intrusion and smaller values to slower cooling. This consistency between cooling rate and ASI value strongly suggests that the intrusion/emplacement process of the Toki granitic magma was effectively affected by the assimilation. Incorporation of country rocks into magma requires a lot of thermal energy to dissolve the country rocks (Glazner 2007). That is, the Toki granite was effectively cooled from the peraluminous regions where assimilation of country rock was most extensive.

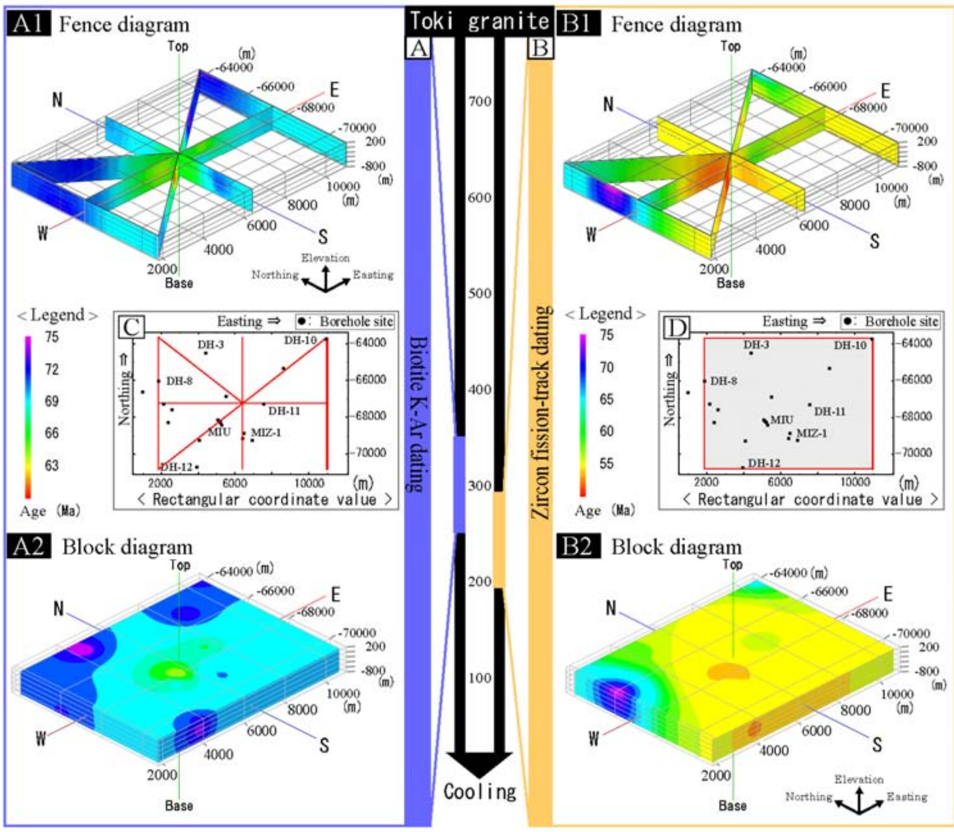


**Fig. 5** Contoured spatial distribution of biotite K-Ar ages (A) and zircon fission track ages (B) in the Toki granite. The fence diagrams (A1 and B1) along the lines on the borehole site map (C), and the block diagrams (A2 and B2) inside the enclosed area in the borehole site map (D) were constructed based on 33 biotite K-Ar age dates and 44 zircon Ft age dates. To make these diagrams, the data were interpolated and converted to 3D data for visualizing of the subsurface geological evidence using Rock Works 14. Northing and easting in the borehole map are expressed based on the rectangular coordinate system with the origin of 137°10’00”E / 36°00’00”N.

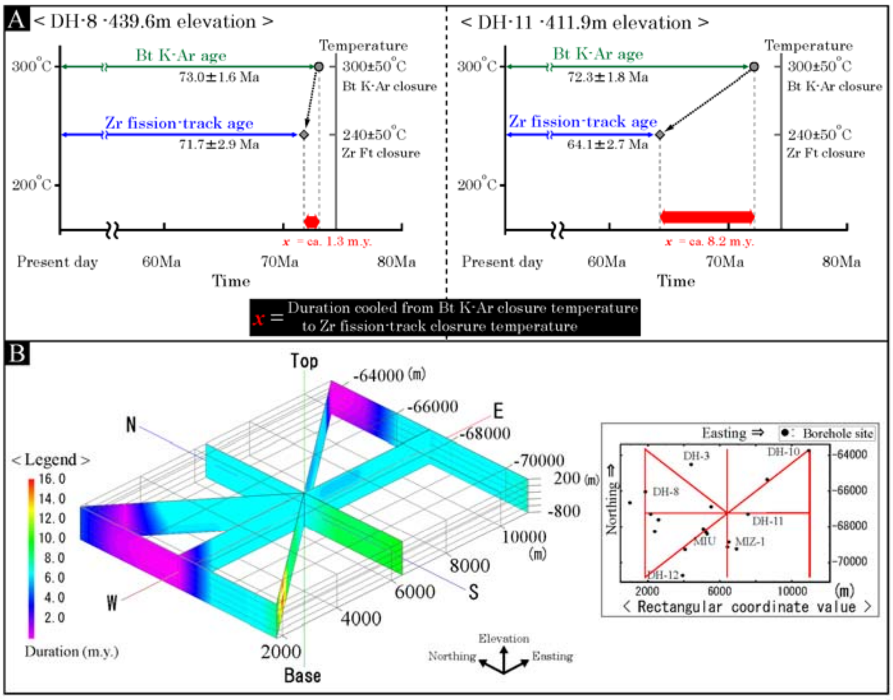


**Fig. 6** Duration of cooling from biotite K-Ar closure temperature (300±50 °C) to zircon fission-track closure (240±50 °C). (A) Example of the duration *x* (1.3 m.y.) at 'DH-8 -439.6 m elevation (northwest margin of the body; left)' and that (8.2 m.y.) at 'DH-11 -411.9 m elevation (central region; right)'. (B) Contoured spatial distribution of the duration of cooling from biotite K-Ar closure temperature to zircon fission-track closure on a fence diagram (using Rock Works 14), based on 33 borehole and outcrop datum.

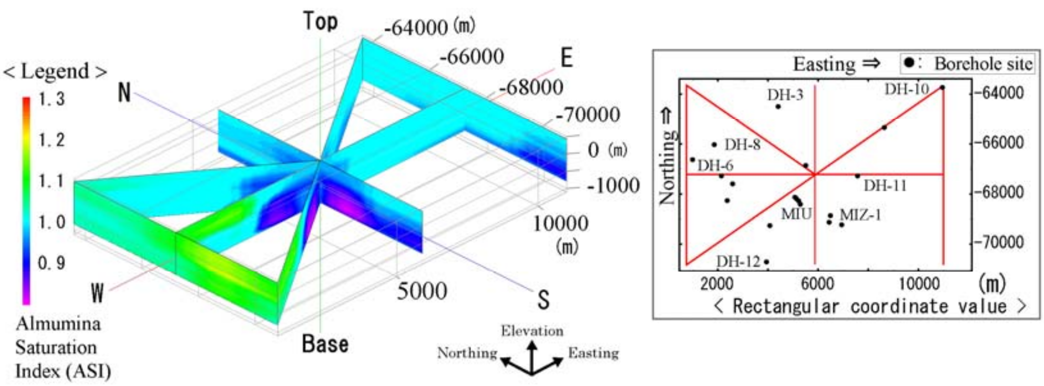


**Fig. 7** Contoured spatial distribution of ASI values on a fence diagram, (using Rock Works 14), based on 483 borehole samples in the Toki granite. Original data (N=483) on the bulk chemical composition are described in Yuguchi et al. (2010).

Contribution to thermal model

Thermal models of granitic cooling have been often discussed numerically (e.g. Okudaira 1996; Scaillet et al. 1996; Annen et al. 2001; Annen 2009 and 2011), which would be useful procedure to acquire the "temporal variation" of cooling pattern of the granitic pluton. Okudaira (1996) described the thermal history of the granitic pluton and its surrounding rocks in the vertical direction by using a 1-D heart transport model. Scaillet et al. (1996) and Annen (2009) presented the 2-D steady-state thermal model of the crust on the cross-section to evaluate the cooling history after the intrusion. The result of numerical model depends largely on a shape of the plutonic body (e.g. thickness and width) and values of parameters (e.g. density, heat capacity, thermal conductivity and latent heart of the plutonic and country rocks, and the heat production rate by radiometric decay in the crust), and hence includes some uncertainty inevitably. In the case of the Toki granite the boundary condition cannot be well defined, because the shape of the body is not well known. It is very difficult in such a case to reveal three-dimensional cooling pattern precisely based on the 3-D numerical model. At this point, multi-sampling thermochronology has a benefit as a practical method to reveal three-dimensional cooling pattern such a granitic body. However, we have to note that the cooling pattern clarified in this study is a "snapshot" of the moment when the Toki granite cooled down to the closure temperature of target mineral.

Memeti et al. (2010) discussed magma chamber evolution of the Tuolumne batholith, Sierra Nevada, California, by a combination of thermochronology (U-Pb zircon age and $^{40}Ar$ / $^{39}Ar$) and 2-D finite difference thermal modeling. Thermochronology shows a 'moment cooling pattern' and thermal model shows a 'temporal variation of cooling pattern'. The combination of the two can give more information for thermal history of the granite body than either one. Our study concludes that the multi-sampling thermochronology provides three-dimensional cooling pattern of the granitic pluton and which is correlated with chemistry (ASI value). Therefore, if both of chronological data and chemistry can be incorporated into numerical model as parameters, it may yield practical thermal model to understand more accurately the temporal change of cooling pattern, which remains as a future study.

## Conclusions

Samples collected from 11 boreholes and seven outcrops in the Toki granite exhibit spatial variations in mineral ages inside the zoned granitic pluton. The result of "multi-sampling thermochronology" based on plural mineral dating with different closure temperatures therefore represents a good indicator of the cooling behavior (cooling pattern and cooling rate) in a granitic pluton. The biotite K-Ar dating and zircon fission-track dating show similar patterns in the Toki granite, giving the central deeper region of the pluton has the youngest ages and the northwest upper margin shows the oldest ages. The region with the older ages corresponds to that of the rapid rate of cooling from biotite K-Ar closure (300±50 $^{o}$C) to zircon fission-track closure (240±50 $^{o}$C), and the region with the younger ages also corresponds to that of the slower cooling rate. Thus, the Toki granite cooled from the roof and the northwest margin of the Toki granite, and then cooling extended to the northeast and further to the central and southern regions. The ASI value becomes larger towards the margin of the Toki granite. There is a strong correlation between the cooling rate and ASI value: large ASI corresponds to more rapid cooling rate, and vice versa. A linkage between the cooling pattern and chemistry is interpreted as that the Toki granite was effectively cooled from the peraluminous regions where assimilation of country rock was most extensive. Thus, the intrusion/emplacement process of the Toki granitic magma was affected by the assimilation. This study combining thermochronology and petrographical methods can delineate a quantitative cooling pattern of a granite at the temperature condition between biotite K-Ar closure and zircon fission-track closure, providing a vital piece of information to reveal the record of the post-kinematic granitic pluton during the period from the intrusion stage, through the sub-solidus stage to the present day.

**Acknowledgements**

The technical comments and English review by Mr. G. McCrank, an ex-JAEA International Fellow, are appreciated. Constructive reviews by Drs. J. Žák, L. Caricchi and J. Blundy (associated editor) were very helpful in revising the manuscript. The authors also thank researchers from the Mizunami Underground Research Laboratory, Japan Atomic Energy Agency, for their discussion and suggestion.

## References


Albarède F (2003) Geochemistry : an introduction. Cambridge University Press, United Kingdom pp 248

Annen C (2009) From plutons to magma chambers: Thermal constraints on the accumulation of eruptible silicic magma in the upper crust. Earth Planet Sci Lett 284: 409-416.

Annen C (2011) Implications of incremental emplacement of magma bodies for magma differentiation, thermal aureole dimensions and plutonism-volcanism relationships. Tectonophysics in press, doi: 10.1016/j.tecto.2009.04.010

Annen C, Lénat J.-F, Privost A (2001) The long-term growth of volcanic edifices: numerical modelling of the role of dyke intrusion and lava-flow emplacement. J Vol Geother Res 105:263-289

Asia Air Survey (1997) Geological Survey on Regional Scale in Tono Area. JNC TJ 2000-027 pp 93 (in Japanese with English Abstract)

Bando M, Bignall G, Sekine K, Tsuchiya N (2003) Petrography and uplift history of the Quaternary Takidani Granodiorite: Could it have hosted a supercritical (HDR) geothermal reservoir? J Volcanol Geotherm Res 120:215-234

Cox A, Dalrymple GB (1967) Statistical analysis of geomagnetic reversal data and the precision of potassium-argon dating. J Geophys Res 72:2603-2614

Dalrymple GB, Lanphere MA (1969) Potassium-Argon Dating; Principles Techniques, and Applications to Geochronology. W. H. Freeman and Co. San Francisco pp 258

Dalrymple GB, Grove M, Lovra OM, Harrison TM, Hulen JB, Lanphere MA (1999) Age and thermal history of the Geysers plutonic complex (felsite unit), Geyers geothermal field, California: a $^{40}$Ar / $^{39}$Ar and U-Pb study. Earth Planet Sci Lett 173:285-298

Danhara T, Iwano H (1983) The zeta age calibration of Fission-track dating. Isotope Geosci 1:285-317

Danhara T, Iwano H, Yoshioka T, Tsuruta T (2003) Zeta calibration values for fission track dating with a diallyl phthalate detector. J Geol Soc Japan 109:665-668 (in Japanese with English abstract)

Dodson H, McClelland-Brown E (1985) Isotopic and paleomagnetic evidence for rates of cooling, uplift and erosion. In: Snelling J (ed) Geological Society of London Memories 10, Oxford, London, pp 315-325

Eby GN, Roden-Tice M, Kyueger HL, Ewing W, Faxon EH, Woolley AR (1995) Geochronology and cooling history of the northern part of the Chilwa Alkaline Province, Malawi. J African Earth Sci 20:275-288

Fujii Y (2000) Fracture analysis of the Toki Granite in the Tono district, central Japan. J Geol Soc Japan 106:249-263 (in Japanese with English abstract)

Glazner AF (2007) Thermal limitations on incorporation of wall rock into magma. Geology 35:319-322

Gleadow AJW (1981) Fission-track dating methods: what are the real alternatives? Nuclear Tracks: Methods, Instruments and Applications 5:3-14

Gleadow AJW, Lovering JF (1977) Geometry factor for external detectors in fission track dating. Nucl Track Detect 1: 99-106

Gleadow AJW, Hurford AJ, Quaife RD (1976) Fission track dating of zircon: improved etching techniques. Earth Planet Sci Lett 33:273-276

Harayama S (1992) Youngest exposed granitoid pluton on Earth: Cooling and rapid uplift of the Pliocene - Quaternary Takidani Granodiorite in the Japan Alps, central Japan. Geology 20:657-660

Harayama S (1994) Cooling history of the youngest exposed pluton in the world – The Plio-Pleistocene Takidani Granodiorite (Japan Alps, central Japan) –. Mem Geol Soc Japan 43:87-97 (in Japanese with English abstract)

Hurford AJ, (1986) Cooling and uplift patterns in the Lepontine Alps South Central Switzerland and an age of vertical movement on the Insubric fault line. Contrib Mineral Petrol 92:413-427

Hurford AJ (1990a) Standardization of fission track dating calibration: Recommendation by the Fission Track Working group of the I.U.G.S. Subcommission of Geochronology. Chem Geol 80:171-178

Hurford AJ (1990b) International Union of Geological Science Subcommission on Geochronology recommendation for the standardization of fission track dating calibration and data reporting. Nuclear Track & Radiat Measurements. 17:233-236

Hurford AJ, Green PF (1983) The zeta age calibration of Fission-track dating. Isotope Geosci 1:285-317

Ishihara S (2003) Chemical contrast of the Late Cretaceous granitoids of the Sanyo and Ryoke Belts, Southwest Japan: Okayama-Kagawa Transect. Bull Geol Surv Japan 54:95-116

Ishihara S, Chappell B (2007) Chemical compositions of the late Cretaceous Ryoke granitoids of the Chubu District, central Japan – Revisited. Bull Geol Surv Japan 58:323-350

Itoigawa J (1974) Geology of the Mizunami district, central Japan. Bull Mizunami Fossil Museum 1:9-42 (in Japanese)

Itoigawa J (1980) Geology of the Mizunami district, central Japan. Monogr Mizunami Fossil Museum 1:1-50 (in Japanese)

Japan Nuclear Cycle Development Institute (2000) Regional Hydrogeological Study Project Result from 1992-1999. JNC Technical Report, JNC TN7400 2003-007, Tono Geoscience Center, pp 86

Japan Nuclear Cycle Development Institute (2002) Master Plan of the Mizunami Underground Research Laboratory Project. JNC Technical Report, JNC TN7410 2003-001, Tono Geoscience Center, pp 47

Memeti V, Paterson S, Matzel J, Mudil R, Okaya D (2011) Magmatic lobes as “snapshots” of magma chamber growth and evolution in large, composite batholiths: An example from the Tuolumne intrusion, Sierra Nevada, California. Geol Soc Amer Bull 24:1912-1931

Oikawa T, Umeda K, Kanazawa S, Matsuzaki T (2006) Unusual cooling of the Middle Miocene Ichifusayama Granodiorite, Kyushu, Japan. J Mineral Petrol Sci 101:23-28

Ota K, Amano K, Suyama Y, Saegusa H (1999) 3D Geological Modelling in Regional Hydrogeological Study in the Tono Area. JNC technical review, 4:101-110

Okudaira T (1996) Thermal evolution of the Ryoke metamorphic belt, southwestern Japan: tectonic and numerical modeling. Island Arc 5:373–385

Pitcher WS (1997) The Nature and Origin of Granite, Second edition. Chapman and Hall, London, pp 408

Sano H, Yamagata T, Horibo K (1992) Tectonostratigraphy of Mino terrane: Jurassic accretionary complex of southwest Japan. Palaeogeography, Palaeoclimatology, Palaeoecology 96:41-57

Scaillet S, Cuney M, Carlier de Veslud C, Cheilletz A, Royer J.J. (1996) Cooling pattern and mineralization history of the Saint Sylvestre and western Marche Leucogranite pluton, French Massif Central: II. Thermal modelling and implications for the mechanisms of uranium mineralization. Geochim Cosmochim Act 60: 4673-4688

Shibata K, Ishihara S (1979) Rb-Sr whole-rock and K-Ar mineral ages of granitic rocks in Japan. Geochem J 13:113-119

Sonehara T, Harayama S (2007) Petrology of the Nohi Rhyolite and its related granitoids: A Late Cretaceous large silicic igneous field in central Japan. J Volcanol Geotherm Res 167:57–80

Steiger RH, Jäger E (1977) Subcommission on geochronology: Convention on the use of decay constants in geo- and cosmochronology. Earth Planet Sci Lett 36:359-362

Suzuki K, Adachi M (1998) Denudation history of the high T/P Ryoke metamorphic belt, southwest Japan: constraints from CHIME monazite ages of gneisses and granitoids. J Metamor Geol 16:27-37

Suzuki K, Nakazaki M, Adachi M (1998) An 85±5 Ma CHIME age for the Agigawa welded tuff sheet in the oldest volcanic sequence of the Nohi Rhyolite, central Japan.

J Earth Planet Sci, Nagoya University, 45:17-27

Tsuchiya N, Fujino K (2000) Evaluation of cooling history of the quaternary Takidani pluton using thermoluminescence technique. Proc World Geothermal Congress 2000, 3939-3944

Umeda K, Komatsu R, Tanase A, Yusa Y (2001) Cooling history of the Takahama Granitic Rocks, Shikoku, Ryoke Belt, Southwest Japan, with special reference to the thermal effect of the Neogene intrusive rocks. Japanese Mag Mineral Petrol Sci 30:17-27 (in Japanese with English abstract)

Yamada N, Wakita K, Hiroshima T, Komazawa T (1990) Geology of the Iida district. With Geological Sheet Map at 1 : 200,000. Geological Survey of Japan, pp 111 (in Japanese with English abstract)

Yamashita N, Kasuno Y, Itoigawa J (1988) Japanese geology 5, Chubu district II. Kyoritsu shuppan, Tokyo, pp 310 (in Japanese)

Yuguchi T, Tsuruta T, Nishiyama T (2010) Zoning of rock facies and chemical composition in the Toki granitic body, Central Japan. Japanese Mag Mineral Petrol Sci 39:50-70 (in Japanese with English abstract)

Yuguchi T, Tsuruta T, Nishiyama T (in prep.A) The spatial distribution of initial $^{87}Sr$ / $^{86}Sr$ ratios inside the Toki granite, Central Japan: Implication for the intrusion and cooling process of a granitic pluton.

Yuguchi T, Amano K, Tsuruta T, Danhara T, Iwano H, Nishiyama T (in prep.B) Three-dimensional cooling history of a granitic pluton over the wide sub-solidus temperature range: The study of multi-sampling thermochronology employing apatite fission-track dating in the Toki granite, Central Japan.

Yuhara M, Kagami H (1995) Cooling history of the Katsuma quartz diorite in the Ina district of the Ryoke belt, Southwest Japan Arc. J Geol Soc Japan 101:434-442

Zhao Z, Zheng Y, Wei C, Gong B (2004) Temporal relationship between granite cooling and hydrothermal uranium mineralization at Dalongshan in China: a combined radiometric and oxygen isotopic study. Ore Geol Rev 25:221-236